Supplement of Atmos. Chem. Phys., 21, 11545–11562, 2021
https://doi.org/10.5194/acp-21-11545-2021-supplement

Atmospheric Chemistry and Physics
Open Access
EGU

Supplement of

Temperature and volatile organic compound concentrations as controlling factors for chemical composition of α-pinene-derived secondary organic aerosol

Louise N. Jensen et al.

Correspondence to: Merete Bilde (bilde@chem.au.dk)

S1-S11 provides explanation for the choice of the four-factor solution of the PMF analysis to be evaluated in the main text.

First of all S1 shows that going from one to four factors significantly reduces the $Q/Q_{expected}$ while increasing the number of factors to five or six leads to a smaller decrease in the $Q/Q_{expected}$. Based on that, in the following focus will primarily be on the four, five and six-factor solutions - and clarify why the four-factor solution is chosen over the five-factor and six-factor solutions.

S2-S4 show the scaled residuals of the four, five and six-factor solutions, respectively. By increasing the number of factors beyond four, reductions in scaled MS residuals are observed, e.g. at some intense m/z's like m/z 43 and m/z 91, but these residuals are still large even for the six-factor solution, indicating that variability at these ions remain unresolved. The same picture is revealed in S5 depicting the variance of the scaled residuals for the three to six factor solutions.

For all the experiments included in the PMF analysis, S6 depicts the time series of the variance in the scaled residuals for the one-factor to six-factor solutions. This figure shows that in general the decrease in scaled residuals by choosing the five or six-factor solution is most significant in the 50 ppb α-pinene experiments (3.1-3.3).

S7 is an un-stacked version of the four-factor solution to the PMF analysis shown in Figure 2 in the main text. More specifically, the mass evolution of each factor during each of the experiments is shown.

Additional sources of uncertainty that are not accounted for in the PMF analysis of high-resolution mass spectra are uncertainties related to HR fitting, including errors in peak shape, and m/z calibrations (Cubison et al., 2015).

The five-factor and six-factor solutions to the PMF analysis are shown in S8-S11 as time series of the mass evolution of the factors and mass spectra of the factors. By comparing these to the four-factor solution (Figures 2 and 3 in the main text) increasing the number of factors in the solution from four to six does not provide increased interpretability. For example, the six-factor solution splits each of the high and low temperature factors, identified in the four-factor solution, into two such that the factors in the six-factor solution can be associated with experimental conditions in the following way:

High temperature factors: Factor 2 and Factor 6

Low loading factor: Factor 3

High loading factor: Factor 4

Low Temperature factor: Factor 1 and Factor 5

The splittings of the factors cannot be uniquely correlated with changes in experimental conditions and therefore they do not provide any more interpretable information about the composition. Based on this and the evaluation of S1-S7, showing that going from to five factors only slightly improves the quality of the analysis, we choose the simpler, more interpretable, four-factor solution.

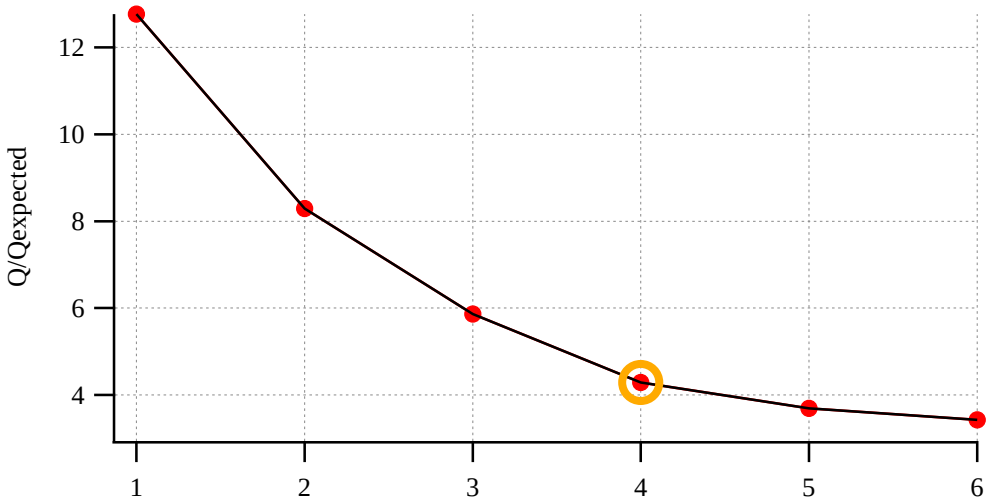

S1. $Q/Q_{expected}$ diagnostic plot from PMF analysis of the combined dataset of experiments 1.1-1.5 and 3.1-3.3. It shows that $Q/Q_{expected}$ of the four-factor solution is 4.3. For the five-factor and six-factor solutions it is slightly lower.

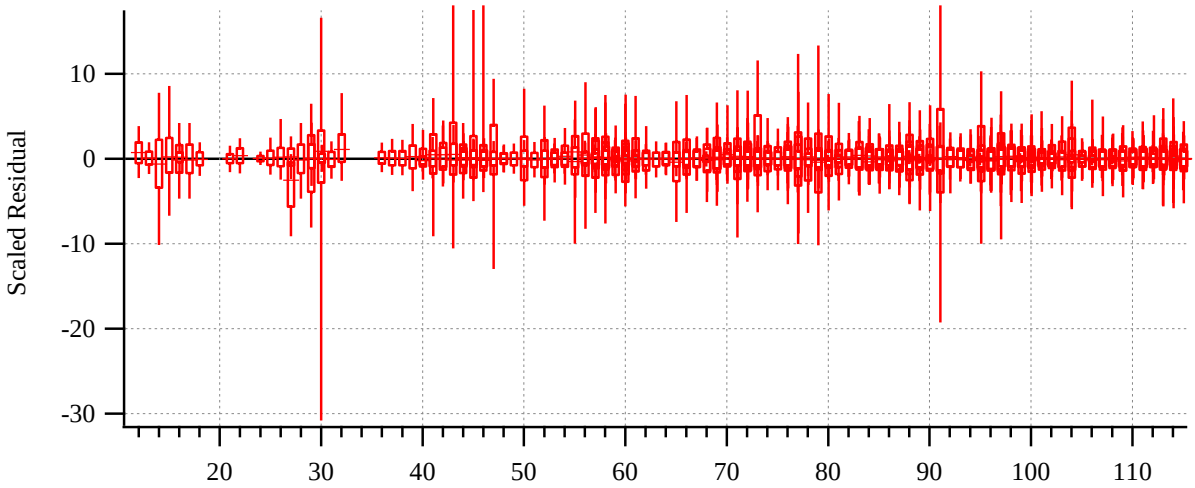

S2. Scaled residuals of all m/z from the four-factor solution of the PMF analysis of the combined datasets of experiments 1.1-1.5 and 3.1-3.3.

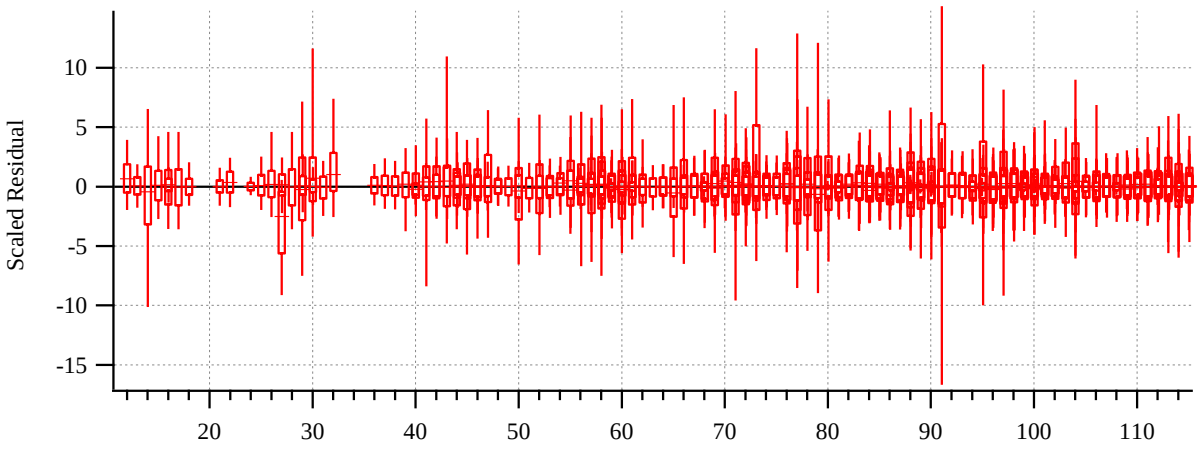

S3. Scaled residuals of all m/z from the five-factor solution of the PMF analysis of the combined datasets of experiments 1.1-1.5 and 3.1-3.3.

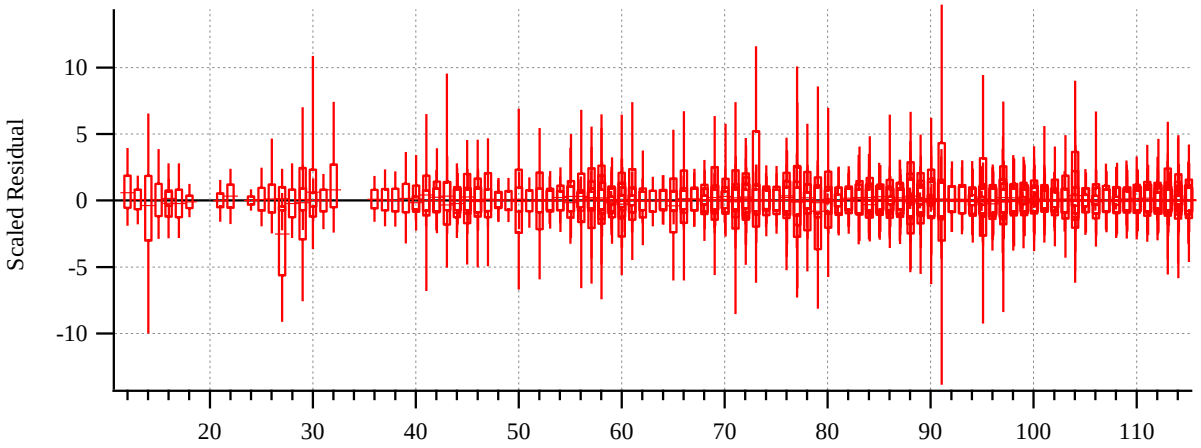

S4. Scaled residuals of all m/z from the six-factor solution of the PMF analysis of the combined datasets of experiments 1.1-1.5 and 3.1-3.3.

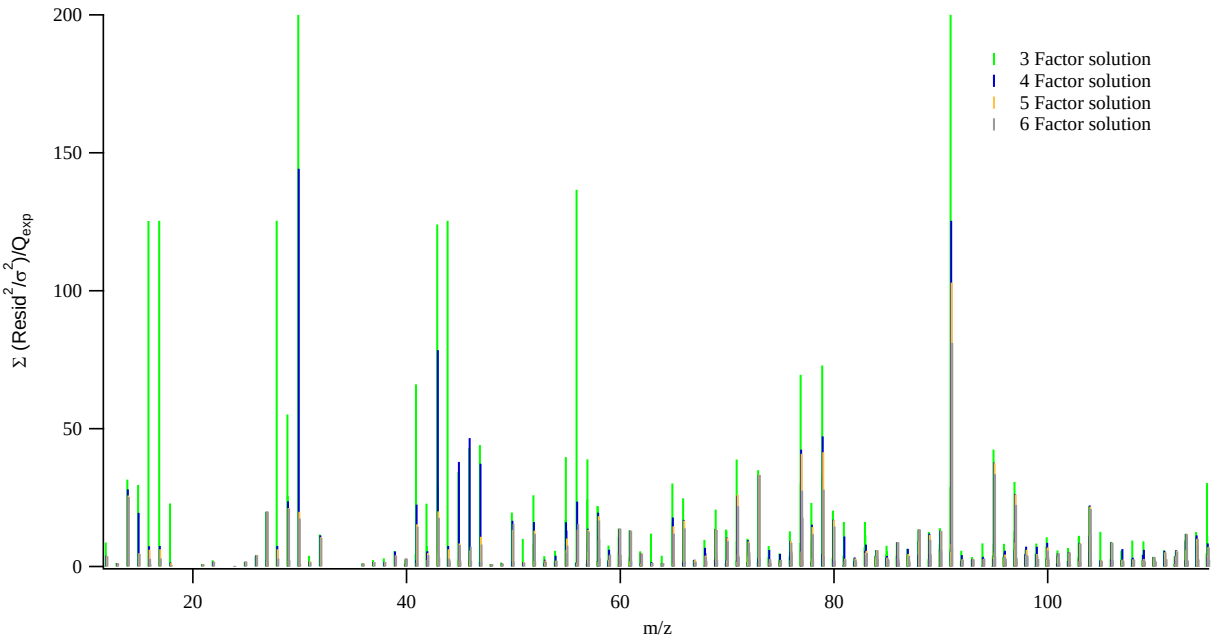

S5. The variance of the residual profiles. Only the three-factor, four-factor, five-factor, and six-factor solutions are shown.

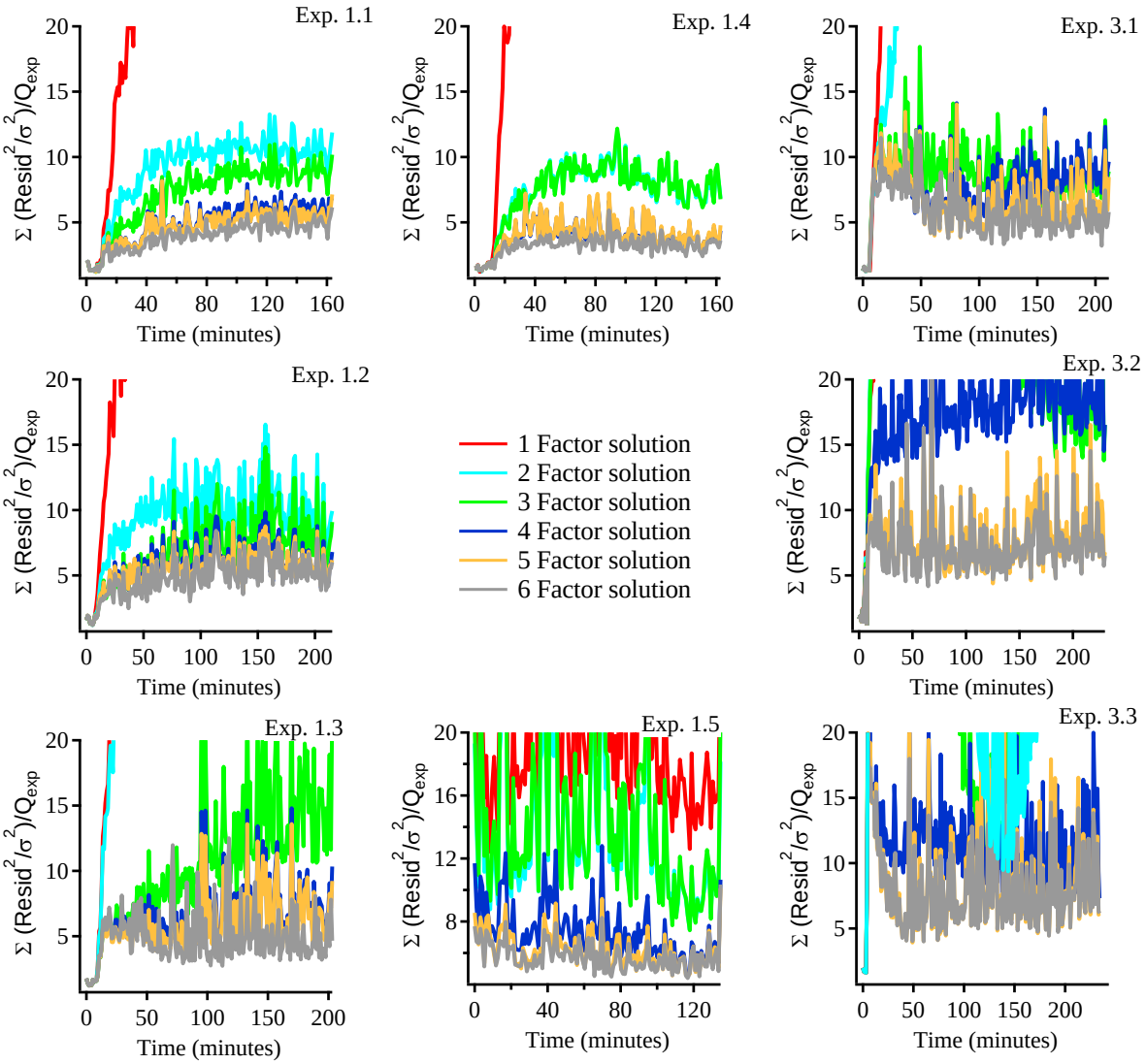

S6. Time series of the variance in the scaled residuals for the one-factor solution to the six-factor solution.

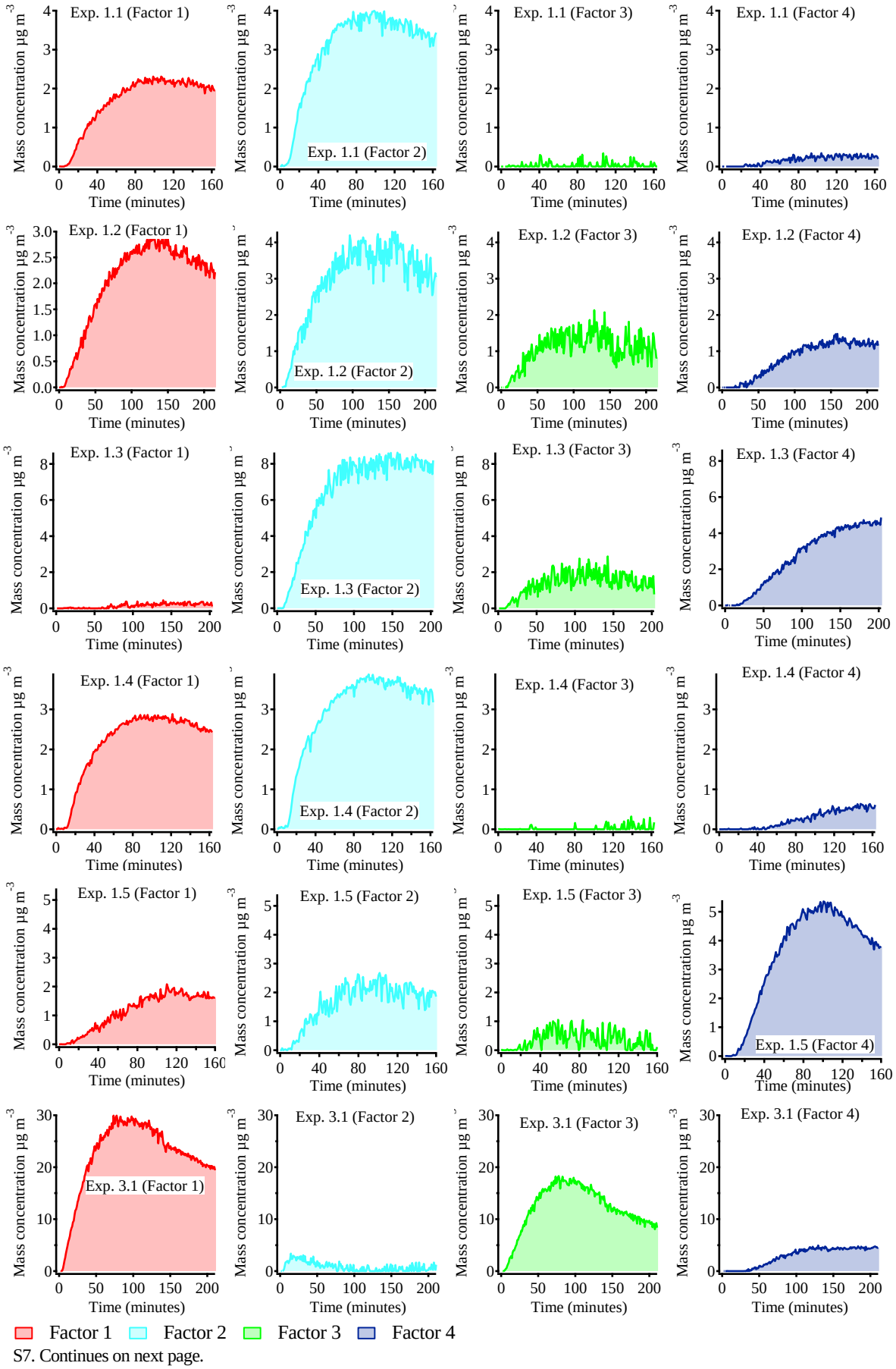

S7. Continues on next page.

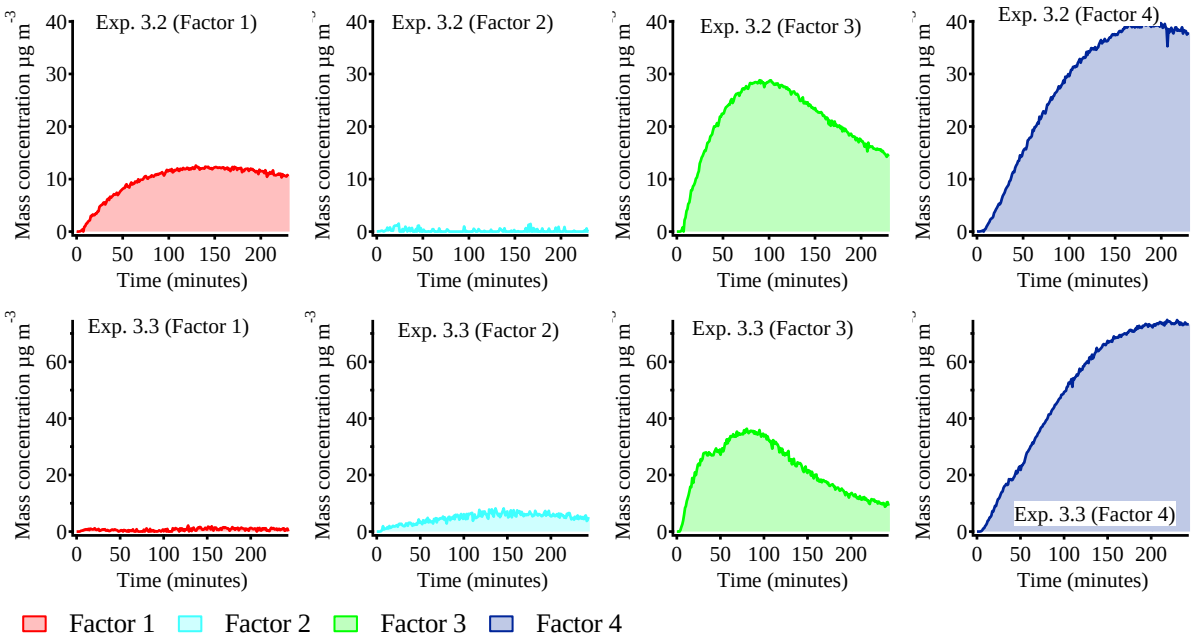

S7. Time series of the four-factor solution to the PMF analysis, depicted as the mass evolution of each of the four factors in each of the experiments (1.1-1.5 and 3.1-3.3) included in the analysis.

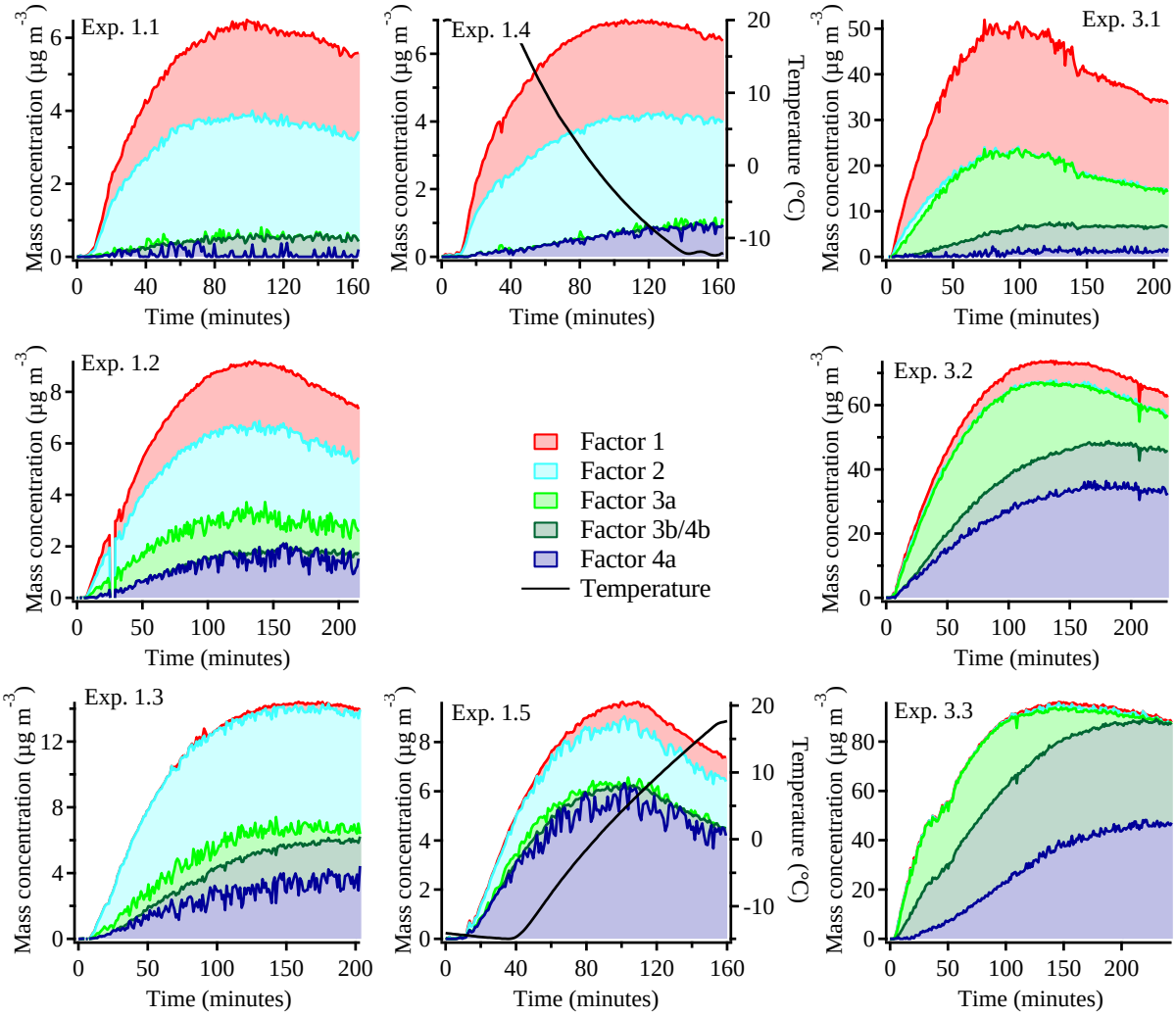

S8. Time series of the mass concentration of the factors obtained in the five-factor solution to the PMF analysis of the combined dataset of experiments 1.1-1.5 and 3.1-3.3.

S9. Mass spectra of five-factor solution from PMF analysis of the combined datasets of experiments 1.1-1.5 and 3.1-3.3.

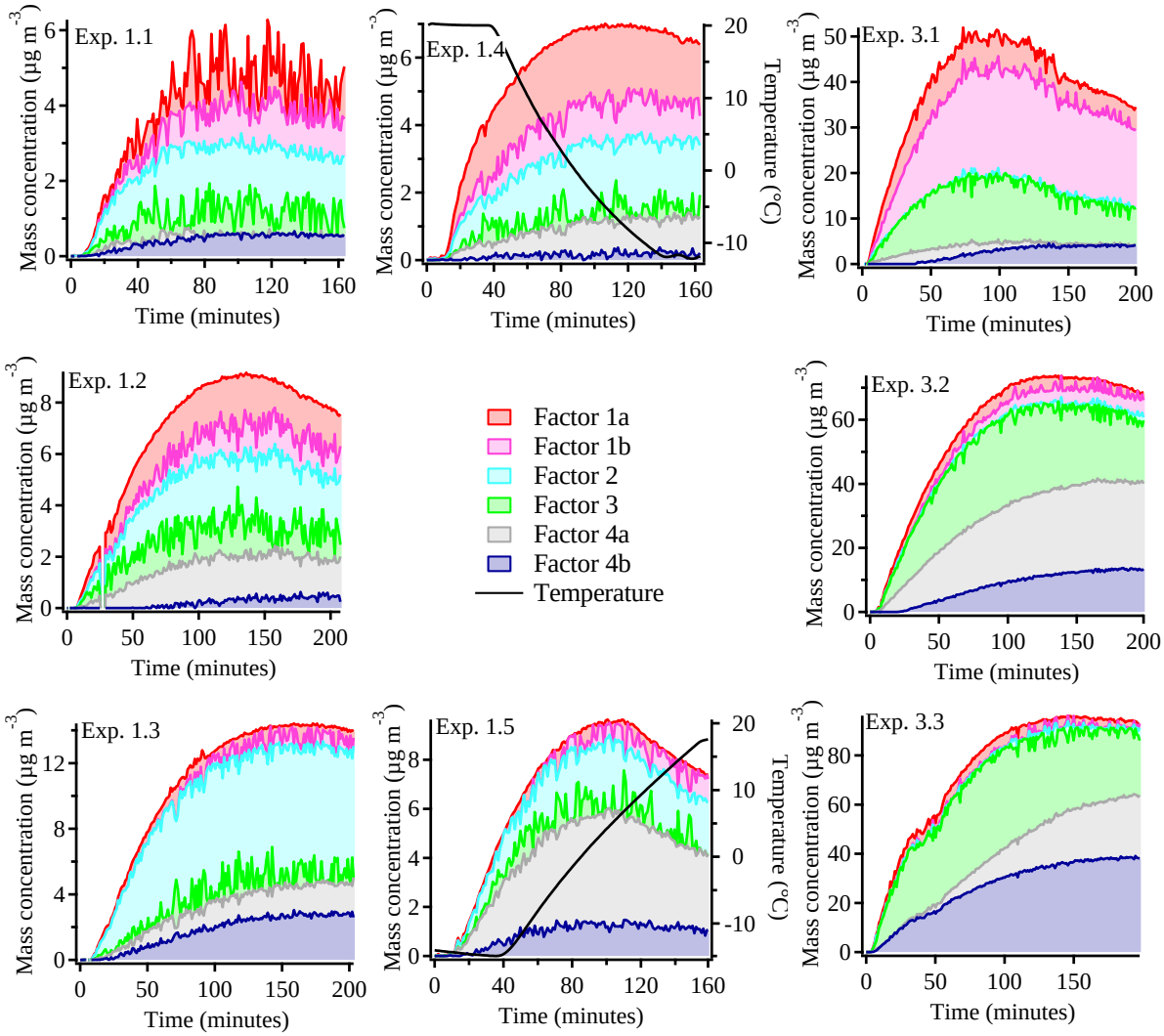

S10. Time series of the mass concentration of the factors obtained in the six-factor solution to the PMF analysis of the combined dataset of experiments 1.1-1.5 and 3.1-3.3.

S11. Mass spectra of six-factor solution from PMF analysis of the combined datasets of experiments 1.1-1.5 and 3.1-3.3.

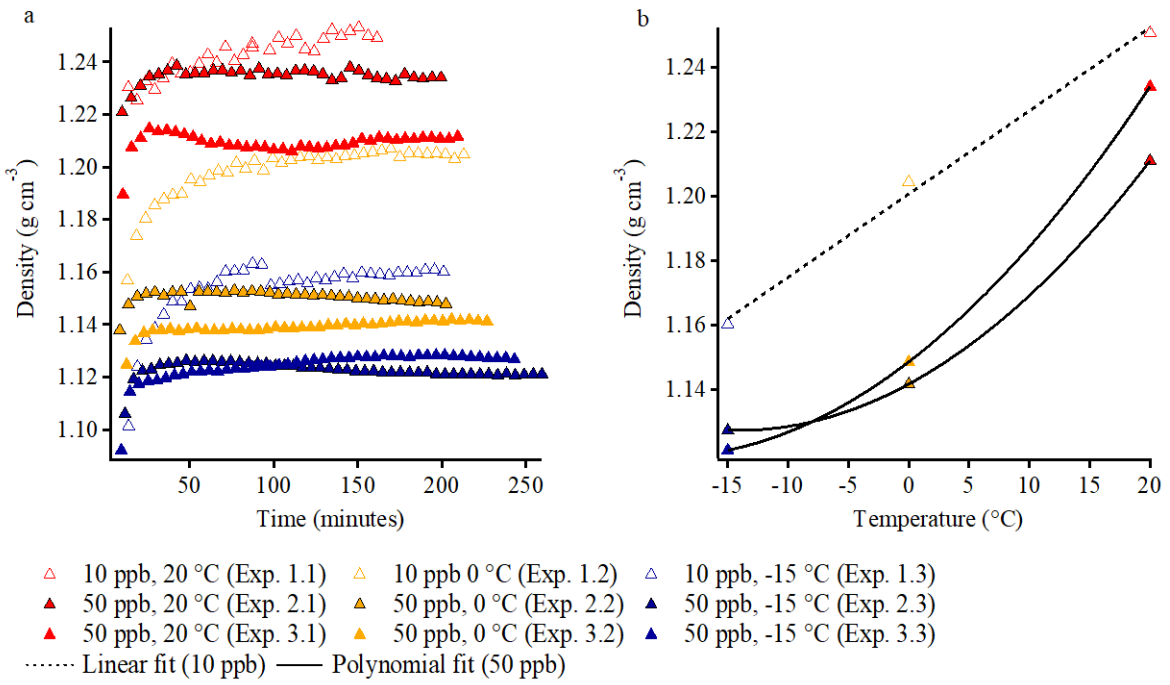

S12. (a) The density of the of SOA particles formed during 10 and 50 ppb α-pinene experiments conducted at 20, 0, and -15 °C (five data point averages). For each experiment (b) shows the average density based on the last 30 minutes data. Fittings are added to guide the eye. The densities are calculated from AMS data using the equation described by Kuwata et al. (2011).

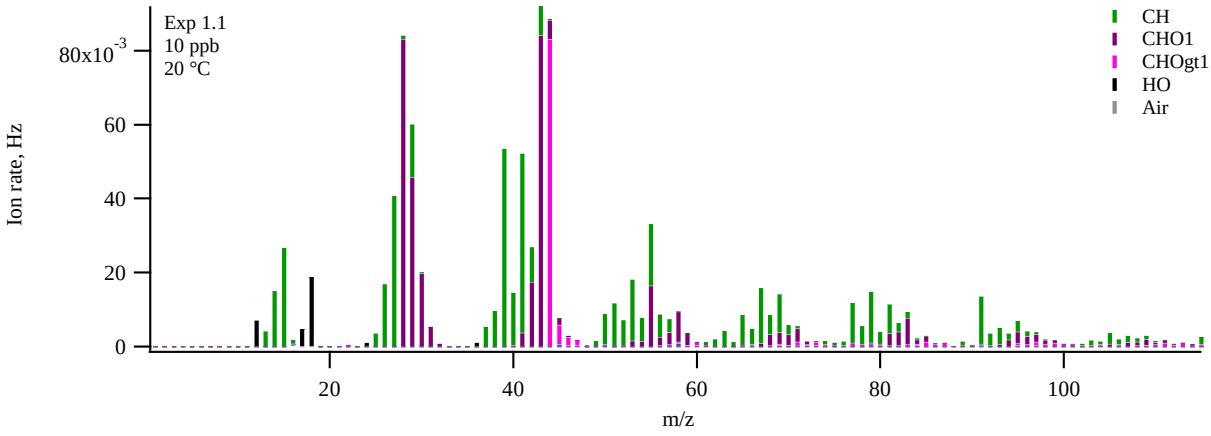

S13. High resolution mass spectrum of experiment 1.1 (based on a five minutes average at mass peak).

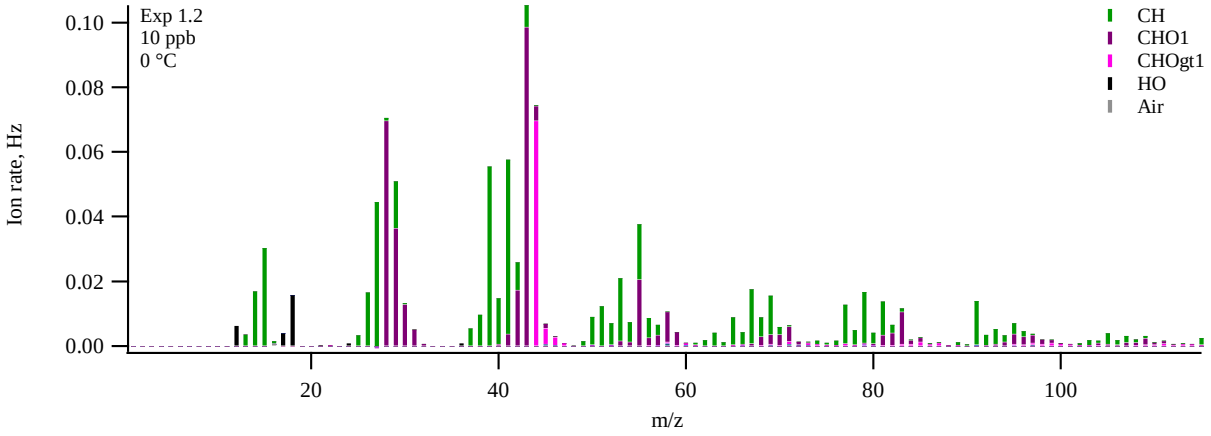

S14. High resolution mass spectrum of experiment 1.2 (based on a five minutes average at mass peak).

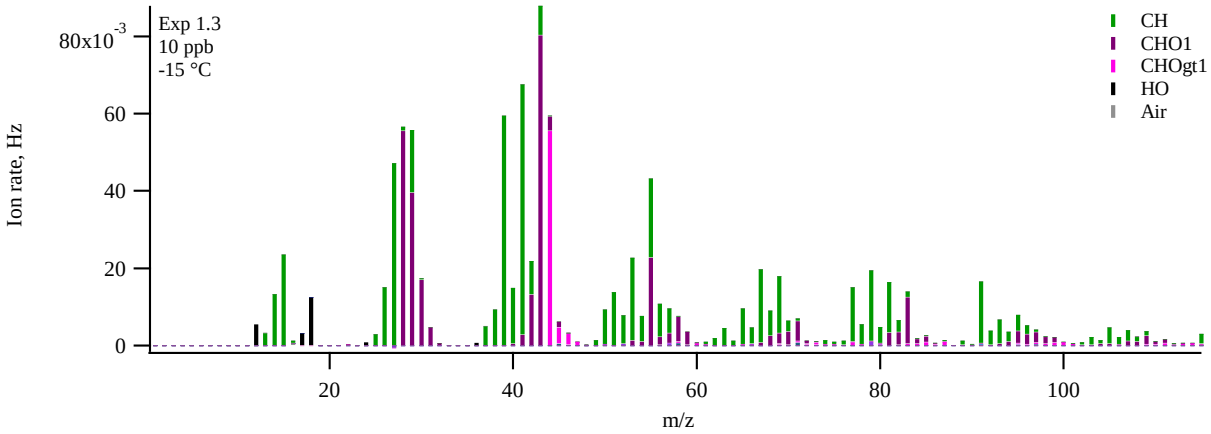

S15. High resolution mass spectrum of experiment 1.3 (based on a five minutes average at mass peak).

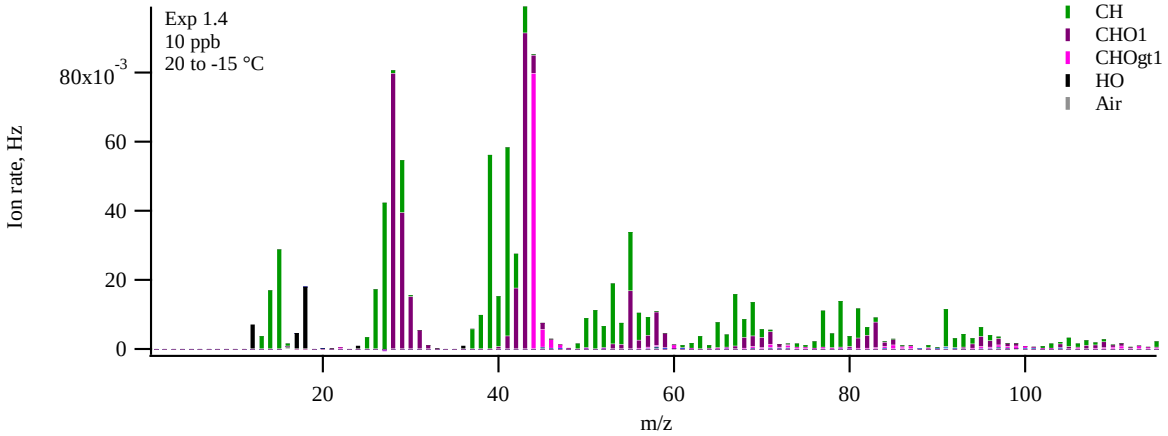

S16. High resolution mass spectrum of experiment 1.4 (based on a five minutes average at mass peak).

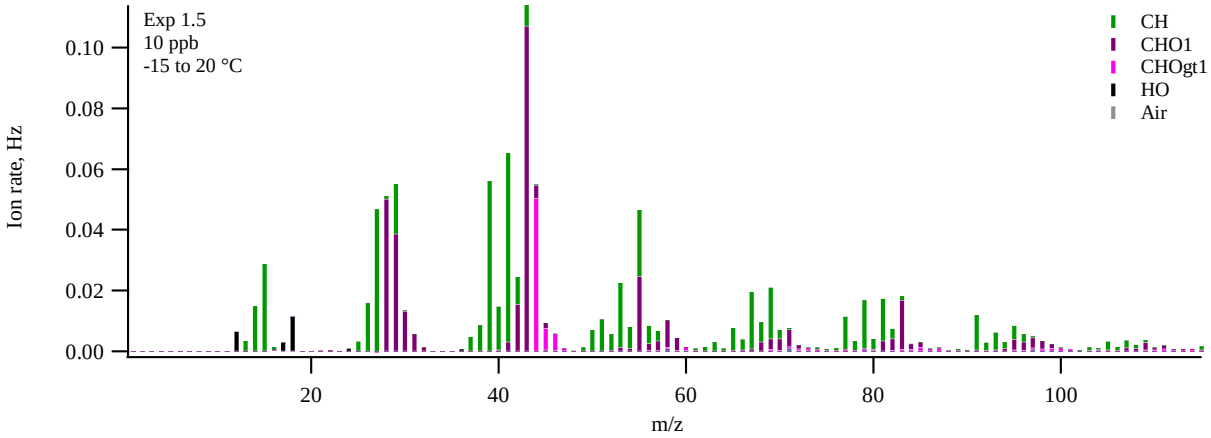

S17. High resolution mass spectrum of experiment 1.5 (based on a five minutes average at mass peak).

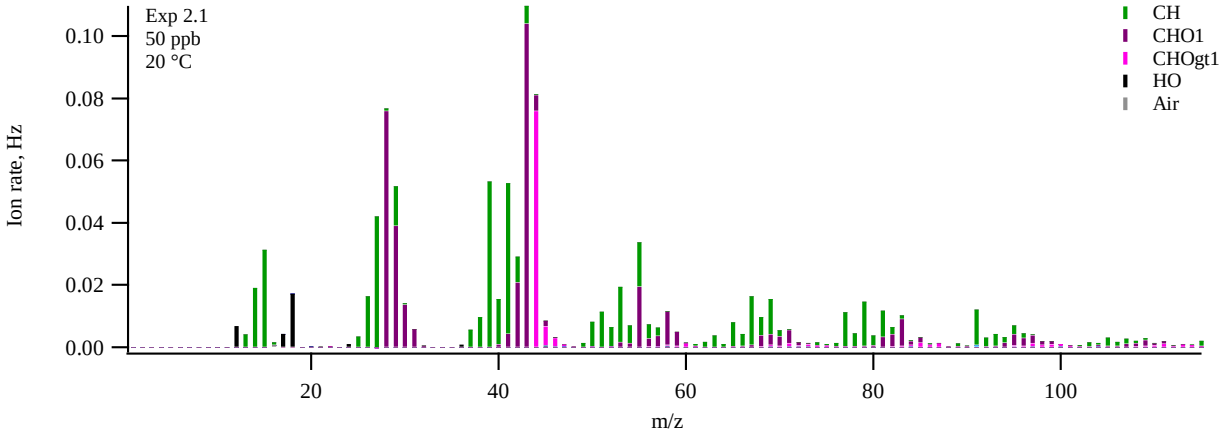

S18. High resolution mass spectrum of experiment 2.1 (based on a five minutes average at mass peak).

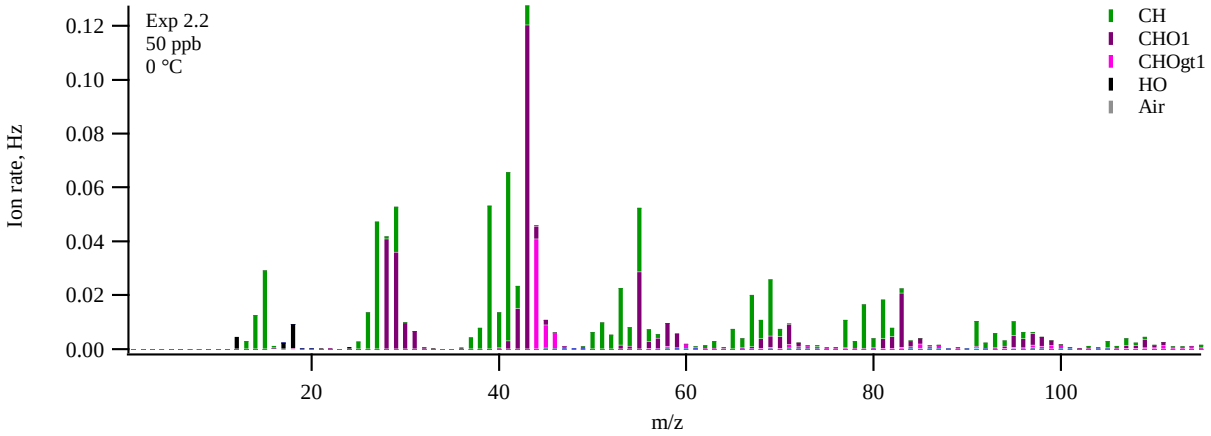

S19. High resolution mass spectrum of experiment 2.2 (based on a five minutes average at mass peak).

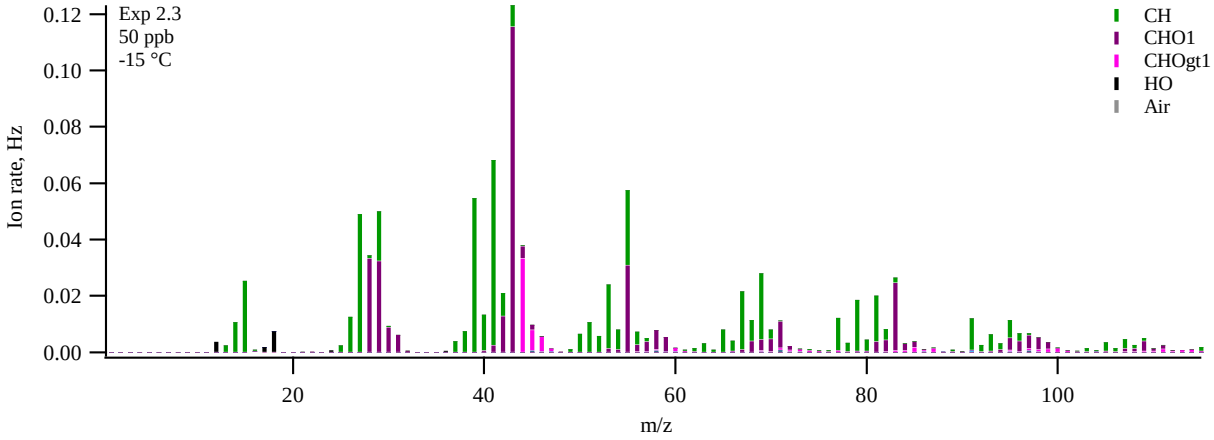

S20. High resolution mass spectrum of experiment 2.3 (based on a five minutes average at mass peak).

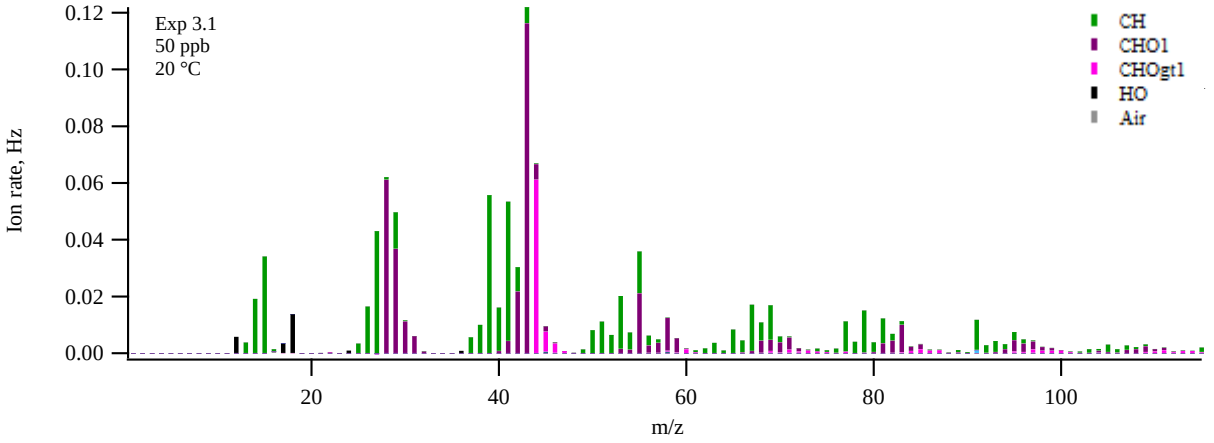

S21. High resolution mass spectrum of experiment 3.1 (based on a five minutes average at mass peak).

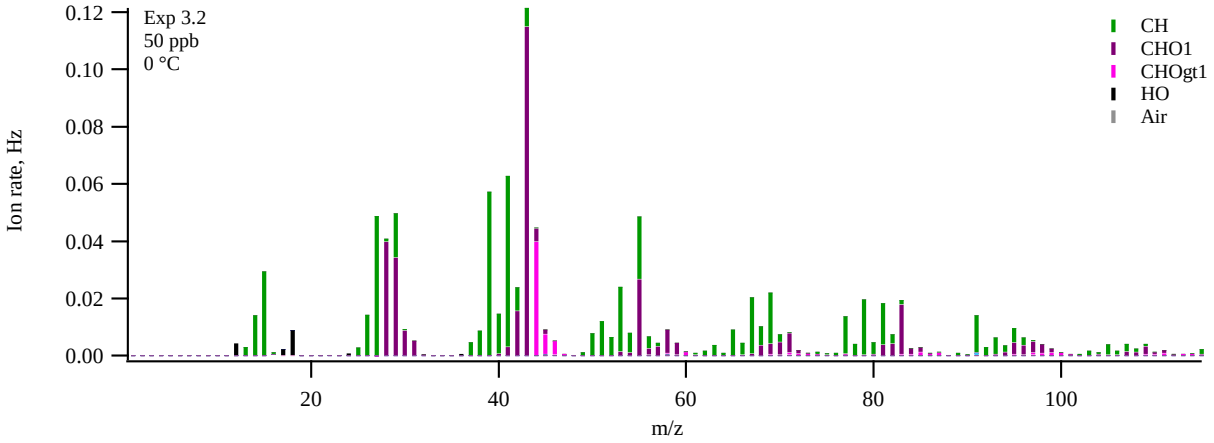

S22. High resolution mass spectrum of experiment 3.2 (based on a five minutes average at mass peak).

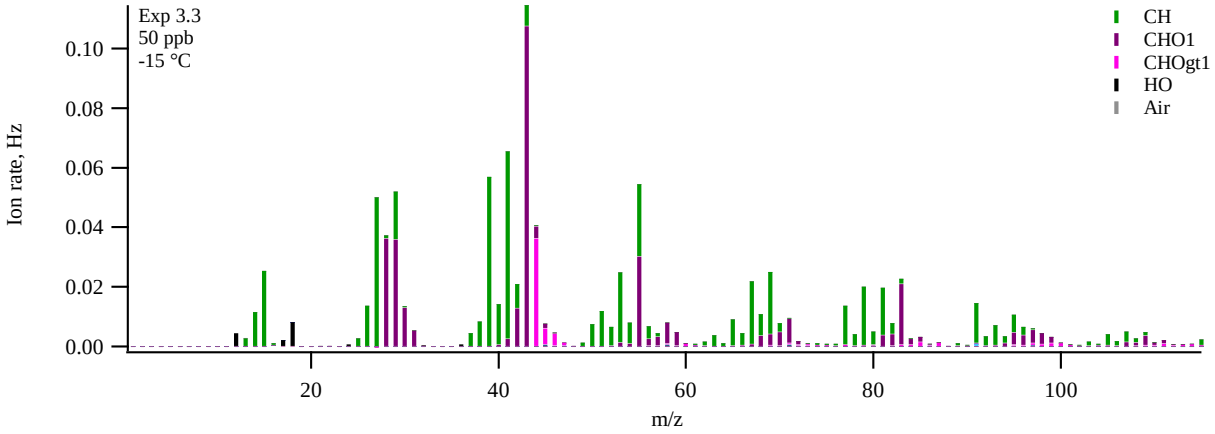

S23. High resolution mass spectrum of experiment 3.3 (based on a five minutes average at mass peak).

S24. Table showing the pairwise similarity of the mass spectra of the four factors from the PMF analysis. The inter comparisons are made using the methods described by both Wan et al. (2002) and Ulbrich et al. (2009). Both methods are applied to both the entire high-resolution m/z range (12-115) and high-resolution m/z > 44. In the method described by Ulbrich et al. (2009) the range of similarity is from 0 to 1 with higher number indicating higher similarity. According to the method presented in Wan et al. (2002), the range is from 0 to 100 with higher number indicating less similarity. In the table green indicates the highest similarity score obtained by each method in a specific m/z range. Red indicates indicates the lowest similarity score obtained by each method in a given m/z range.

Method and m/z range	1 (high T) vs 2 (low C)	1 (high T) vs 3 (high C)	1 (high T) vs 4 (low T)	2 (low C) vs 3 (high C)	2 (low C) vs 4 (low T)	3 (high C) vs 4 (low T)
Ulbrich et al. all m/z	0.90	0.86	0.89	0.89	0.87	0.97
Ulbrich et al. m/z > 44	0.85	0.86	0.89	0.97	0.87	0.91
Wan et al. all m/z	54.04	53.36	47.57	52.22	52.95	46.22
Wan et al. m/z > 44	56.91	55.75	49.41	54.71	55.51	49.14

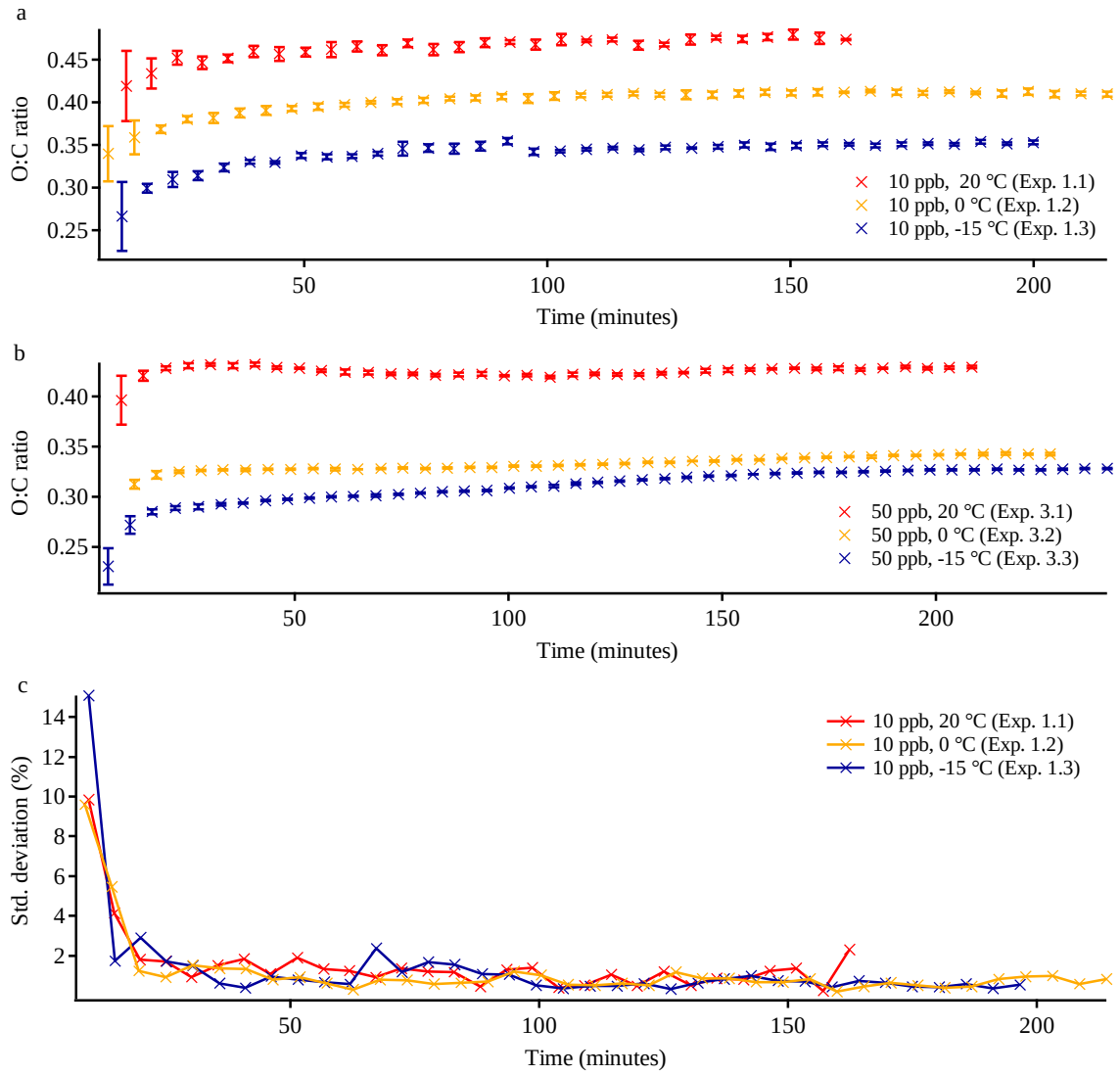

S25. Standard deviations of the O:C ratios obtained in (a) the 10 ppb α-pinene experiments conducted at 20, 0, and -15 °C (experiments 1.1-1.3), and (b) the 50 ppb α-pinene experiments conducted at 20, 0, and -15 °C (experiments 3.1-3.3). (c) shows the standard deviation of the 10 ppb α-pinene experiments (1.1-1.3) in percentages.

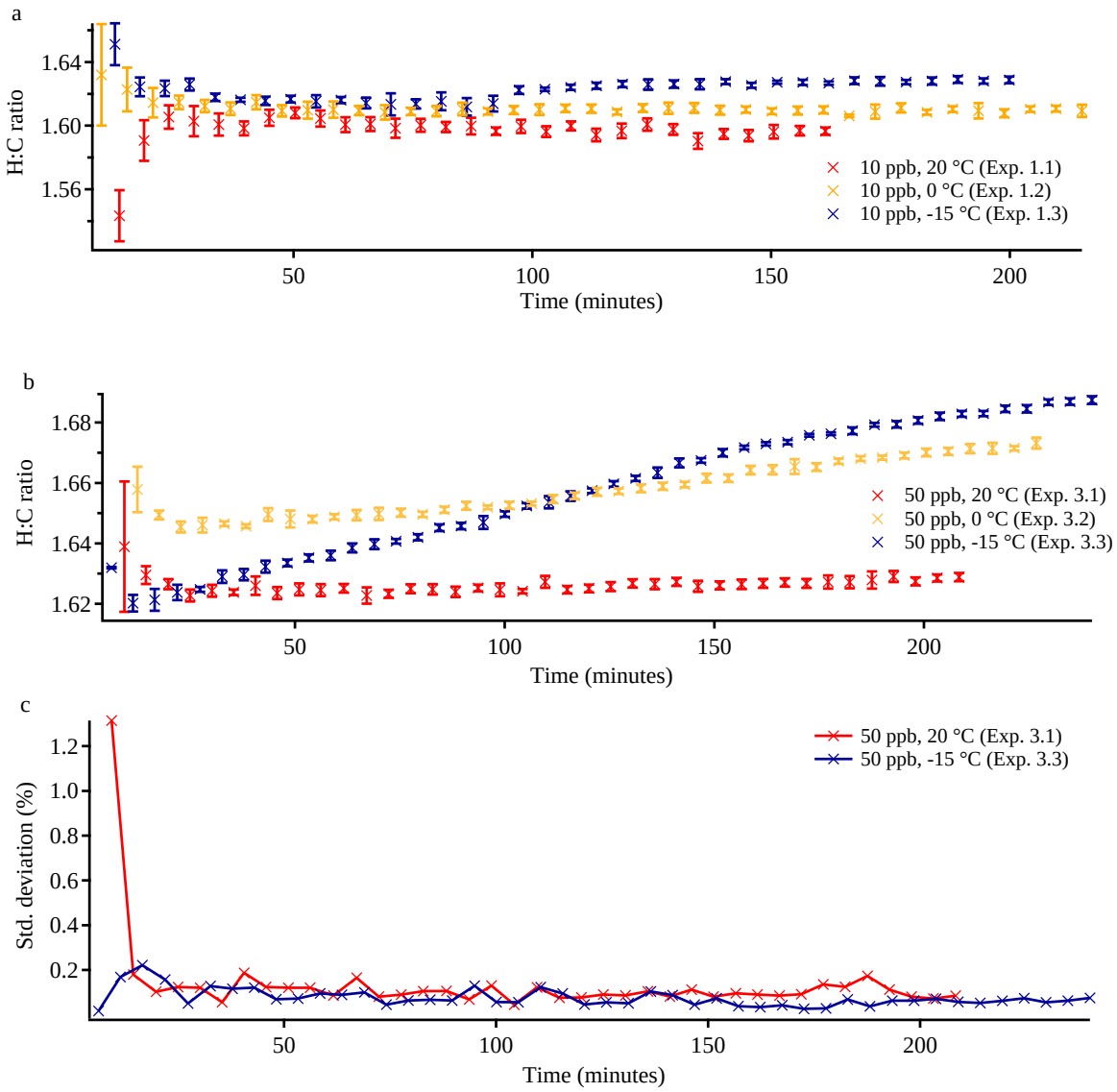

S26. Standard deviations of the H:C ratios obtained in (a) the 10 ppb α-pinene experiments conducted at 20, 0, and -15 °C (experiments 1.1-1.3), and (b) the 50 ppb α-pinene experiments conducted at 20, 0, and -15 °C (experiments 3.1-3.3). (c) shows the H:C ratio standard deviation of the 50 ppb α-pinene experiments conducted at -15 and 20 °C (experiments 1.1 and 1.3) in percentages.

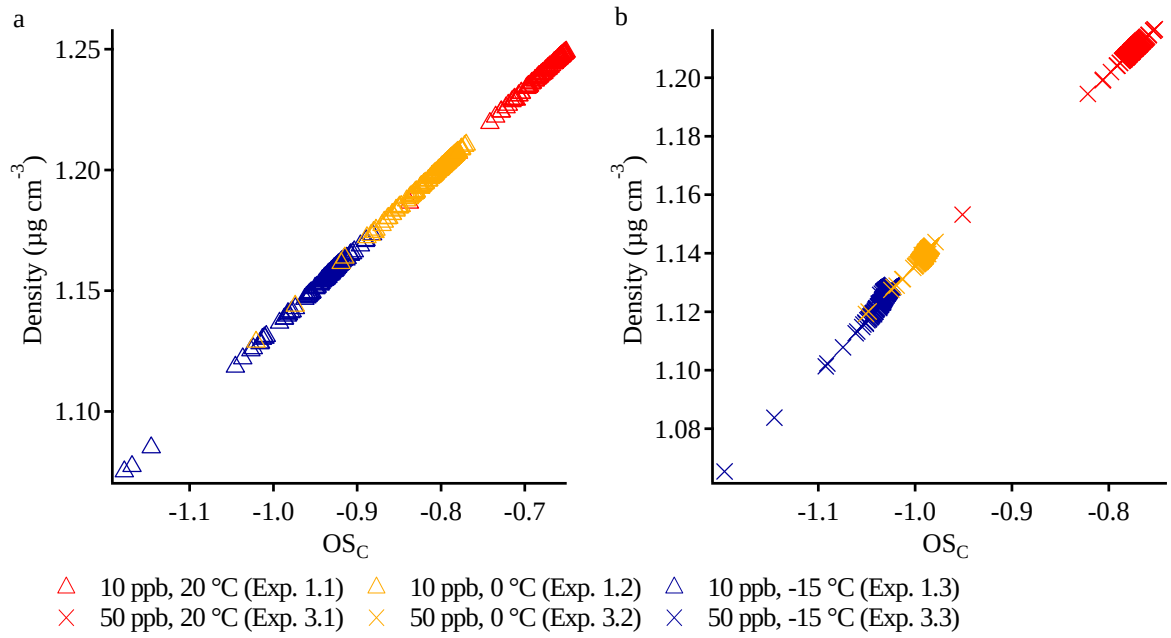

S27. The correlation between OS_C and density of the SOA formed in at 20, 0, and -15 °C experiments initiated at (a) 10 ppb α-pinene and (b) 50 ppb α-pinene. The densities are calculated from AMS data using the equation described by Kuwata et al. (2011) and OS_C is calculated as described by Kroll et al. (2011).

References

Cubison, M.J. and Jimenez, J.L., 2015. Statistical precision of the intensities retrieved from constrained fitting of overlapping peaks in high-resolution mass spectra. *Atmospheric Measurement Techniques* (Online), 8(6): 2333-2345.

Kroll, J. H., Donahue, N. M., Jimenez, J. L., Kessler, S. H., Canagaratna, M. R., Wilson, K. R., Altieri, K. E., Mazzoleni, L. R., Wozniak, A. S., Bluhm, H., Mysak, E. R., Smith, J. D., Kolb, C. E. and Worsnop, D. R. 2011. Carbon oxidation state as a metric fordescribing the chemistry of atmospheric organic aerosol, *Nature Chemistry* 3(2): 133-139.

Kuwata, M., S. R. Zorn, and S. T. Martin. 2011. Using elemental ratios to predict the density of organic material composed of carbon, hydrogen, and oxygen. *Environmental science & technology* 46 (2):787-794.

Ulbrich, I. M., M. R. Canagaratna, Q. Zhang, D. R. Worsnop, and J. L. Jimenez. 2009. Interpretation of organic components from Positive Matrix Factorization of aerosol mass spectrometric data. *Atmospheric Chemistry and Physics* 9 (9):2891-2918.

Wan, K. X., Vidavsky, I. and Gross, M. L. 2002. Comparing similar spectra: From similarity index to spectral contrast angle, *Journal of the American Society for Mass Spectrometry.*13(1): 85-88.